

# Molecularly Engineering Defective Basal Planes in Molybdenum Sulfide for the Direct Synthesis of Benzimidazoles by Reductive Coupling of Dinitroarenes with Aldehydes

Miriam Rodenes, Francisco Gonell, Santiago Martín, Avelino Corma,\* and Iván Sorribes\*



Cite This: *JACS Au* 2022, 2, 601–612



Read Online

ACCESS |

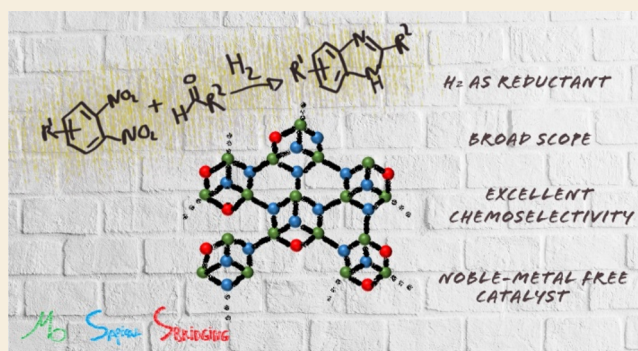
Metrics & More

Article Recommendations

Supporting Information

**ABSTRACT:** Developing more sustainable catalytic processes for preparing N-heterocyclic compounds in a less costly, compact, and greener manner from cheap and readily available reagents is highly desirable in modern synthetic chemistry. Herein, we report a straightforward synthesis of benzimidazoles by reductive coupling of *o*-dinitroarenes with aldehydes in the presence of molecular hydrogen. An innovative molecular cluster-based synthetic strategy that employs Mo<sub>3</sub>S<sub>4</sub> complexes as precursors have been used to engineer a sulfur-deficient molybdenum disulfide (MoS<sub>2</sub>)-type material displaying structural defects on both the naturally occurring edge positions and along the typically inactive basal planes. By applying this catalyst, a broad range of functionalized 2-substituted benzimidazoles, including bioactive compounds, can be selectively synthesized by such a direct hydrogenative coupling protocol even in the presence of hydrogenation-sensitive functional groups, such as double and triple carbon–carbon bonds, nitrile and ester groups, and halogens as well as diverse types of heteroarenes.

**KEYWORDS:** defective molybdenum sulfide, molecular clusters, heterogeneous catalysis, *o*-dinitroarenes, hydrogenative coupling, benzimidazoles



## INTRODUCTION

Benzimidazoles are key heterocyclic scaffolds for drug design in the pharmaceutical industry owing to their remarkable medicinal and pharmacological properties.<sup>1–4</sup> Based on the benzimidazole molecular framework as an essential pharmacophore, several classes of drugs exhibiting antiviral, anticancer, antihypertensive, antihistaminic, antiarrhythmic, and antifungal activities have been developed.<sup>5–7</sup> In addition to their therapeutic uses, benzimidazole derivatives have also been employed as biologically active compounds to prepare pesticides, including fungicides, herbicides, and insecticides, for the agricultural sector.<sup>8</sup> Materials science is another field in which benzimidazoles have found interesting applications as structural subunits for the fabrication of high-performance polymers,<sup>9</sup> adsorbent materials,<sup>10,11</sup> and liquid crystals.<sup>12</sup> Furthermore, they have proved to be an essential core for dye sensitized solar cells,<sup>13</sup> and organic light emitting devices (OLEDs).<sup>14</sup>

In view of these applications, it is not surprising that tremendous efforts have been devoted to the development of methods for preparing these valuable fused heterocycles. In general, the most common methodologies for the synthesis of 2-substituted benzimidazoles rely on using *o*-phenylenediamines as starting materials. The traditional synthesis involves the reaction

of these reagents with carboxylic acid derivatives under strongly acidic conditions, sometimes at high temperature or under microwave irradiation.<sup>15–25</sup> Another conventional method makes use of aldehydes, which led to the formation of the Schiff's bases by condensation reaction with *o*-phenylenediamines, followed by cyclization and aerobic oxidation of the C–N bond to form the target compounds.<sup>26–39</sup> In addition, the metal-catalyzed oxidative<sup>40</sup> or acceptorless dehydrogenative<sup>41–44</sup> coupling of primary alcohols with *o*-phenylenediamines have also been proposed as effective synthetic methods for the preparation of benzimidazoles.

Currently, the quest for sustainable chemistry in organic synthesis has led researchers to develop new synthetic approaches based on domino or tandem processes, in which the preparation of high valuable products takes place through more benign and straightforward multistep one-pot reac-

Received: October 25, 2021

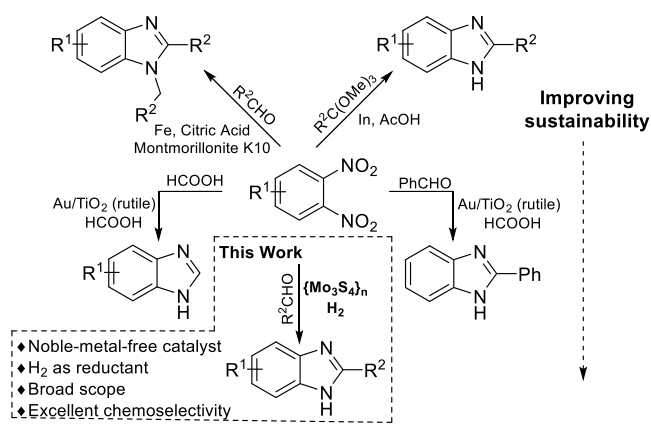
Published: February 9, 2022



tions.<sup>45–53</sup> Nitroarenes are a cheap and readily available feedstock, and their reduction is the method of choice for producing anilines. Therefore, their use as starting reagents for the synthesis of substituted secondary and tertiary aniline derivatives, including aromatic N-heterocyclic compounds, is highly attractive since prior isolation of the primary amines can be avoided. In this regard, more sustainable methodologies to access benzimidazoles have been accomplished by reaction of *o*-nitroanilines with alcohols through a borrowing hydrogen (also called hydrogen autotransfer) mechanism<sup>54–61</sup> or, to a lesser extent, by reductive coupling of these reagents with aldehydes,<sup>62–66</sup> in both cases in the presence of transition metal-based catalysts. Moreover, redox condensation reactions of *o*-nitroanilines with aryl derivatives (alcohols,<sup>67</sup> amines,<sup>68</sup> acetic acids,<sup>69</sup> chlorides<sup>70</sup>) catalyzed by Fe(or Co)/sulfur systems have also been reported.

However, in spite of the evident potential associated with the more straightforward and step economy route of using dinitroarenes as viable starting reagents to access N-heterocyclic compounds,<sup>71–73</sup> the preparation of benzimidazoles from these readily available reactants has so far been scarcely investigated (Scheme 1). Synthetic strategies based on the redox

**Scheme 1. Synthesis of Benzimidazoles from *o*-Dinitroarenes**



condensation of *o*-dinitroarenes with orthoesters or aldehydes to form 2-substituted or 1,2-disubstituted benzimidazoles were established by using an excess of metal (In<sup>74</sup> or Fe<sup>75</sup>) as reductant and acetic or citric acid as the proton source, respectively. Meanwhile, Cao and co-workers reported the reductive N-formylation of *o*-dinitroarenes, catalyzed by an Au/TiO<sub>2</sub> (Rutile) heterogeneous catalyst, in which formic acid is used as both a reductant and a C<sub>1</sub> source.<sup>76</sup> Interestingly, the same group also introduced the synthesis of 2-phenylbenzimidazole as a single example of a transfer hydrogenation coupling reaction of *o*-dinitroarenes with aldehydes using formic acid as a reducing agent.<sup>77</sup>

Nevertheless, besides the limited substrate scope, all these protocols have several drawbacks such as low atom efficiency as well as the use of corrosive acids, excess amounts of metals as reductants, or precious metal-based catalysts. In this respect, the use of the most “green” reductant, *i.e.*, molecular hydrogen, in combination with a noble-metal-free catalyst would provide compelling benefits. However, the implementation of a hydrogenative coupling methodology for preparing benzimidazole derivatives that makes use of dinitroarenes and other readily available reagents, such as for instance aldehydes, remains

elusive mainly due to the need to find efficient catalysts capable of performing this challenging transformation.

Molybdenum sulfides could be promising candidates to catalyze such a direct hydrogenative synthetic strategy. Molybdenum disulfide (MoS<sub>2</sub>)-based materials are key catalysts for hydrotreating processes, performed in the refining industry to eliminate sulfur and nitrogen heteroatoms from crude feedstocks.<sup>78,79</sup> Consequently, extensive work has been done to improve the catalytic activity of this kind of catalysts, and to date, it is an area of continuing interest for the chemical industry and academic research. Within the lamellar structure of MoS<sub>2</sub>, which is constituted by stacked S–Mo–S trilayers, active sites are mainly localized at the edges whereas the basal planes are largely inert.<sup>80–82</sup> More specifically, coordinatively unsaturated sites (CUS), created as sulfur vacancies, and the presence of metal-like electronic states at the brim sites are the proposed active sites of MoS<sub>2</sub>,<sup>83–85</sup> whose number can be significantly increased by adsorption of promoters (such as Co or Ni) at the edge positions of the layered structure.<sup>86–92</sup> Taking advantage of this knowledge, in 2017, we reported the hydrothermal preparation of cobalt-promoted MoS<sub>2</sub> materials and their unprecedented use as catalysts for the chemoselective hydrogenation of nitroarenes to anilines, including dinitro compounds.<sup>93</sup> In the following years, we prepared cobalt–molybdenum sulfides (Co–Mo–S) with tunable phase composition that displayed enhanced catalytic activity for the chemo- and regioselective hydrogenation of quinoline derivatives<sup>94</sup> and for the borrowing hydrogen synthesis of thioethers from alcohols.<sup>95</sup> Later on, bimetallic iron molybdenum selenides were applied as catalysts for the preparation of pyrrolo[1,2-*a*]quinoxalines from *o*-nitroanilines.<sup>96</sup>

In the meantime, nonpromoted MoS<sub>2</sub>-based materials have also been established as efficient catalysts for the reduction of nitroarenes in the presence of different reducing agents, such as hydrazine,<sup>97,98</sup> ammonium formate,<sup>99</sup> or sodium borohydride.<sup>100,101</sup> However, due to the inherent limited catalytic activity of these materials, several strategies were adopted to obtain catalysts with a high degree of active defect sites on both the edges and the typically unreactive basal planes. These strategies involved the preparation of an oxygen-implanted MoS<sub>2</sub> via an incomplete sulfidation and reduction method,<sup>97,99</sup> the Li intercalation/exfoliation to generate the 1T-phase of MoS<sub>2</sub>,<sup>100</sup> a wet-chemical activation with hydrazine of solvent-dispersed 2D-MoS<sub>2</sub> nanosheets,<sup>101</sup> and a carbon insertion to obtain interlayer-expanded MoS<sub>2</sub>.<sup>98</sup> Nevertheless, since hydrogen activation is more challenging, the use of nonpromoted MoS<sub>2</sub>-derived catalysts for the hydrogenation of nitroarenes is quite limited. It was reported that MoS<sub>2</sub>, obtained by atmospheric pressure reduction from MoS<sub>3</sub>,<sup>102</sup> and Zr-intercalated MoS<sub>2</sub><sup>103</sup> catalyzed the conversion of nitrobenzene into aniline in low yield (<40%), a transformation which was later quantitatively accomplished by applying hydrothermally prepared MoS<sub>2</sub> microflowers containing CUS in a high degree.<sup>104</sup> More recently, the catalytic activity of MoS<sub>2</sub>, prepared via a hydrothermal synthesis, was improved by sublimation induced sulfur vacancy creation, and it was applied for the one-pot cascade nitro-hydrogenation and reductive amination for synthesizing secondary amines.<sup>105</sup>

Herein, we report a new bottom-up strategy to obtain a sulfur deficient MoS<sub>2</sub>-type material derived from molecular complexes containing a Mo<sub>3</sub>S<sub>4</sub> cluster core, a class of structural motif that displays structure similarities to MoS<sub>2</sub>, and since Mo<sub>3</sub>S<sub>4</sub> clusters have been shown to catalyze reductive organic transforma-

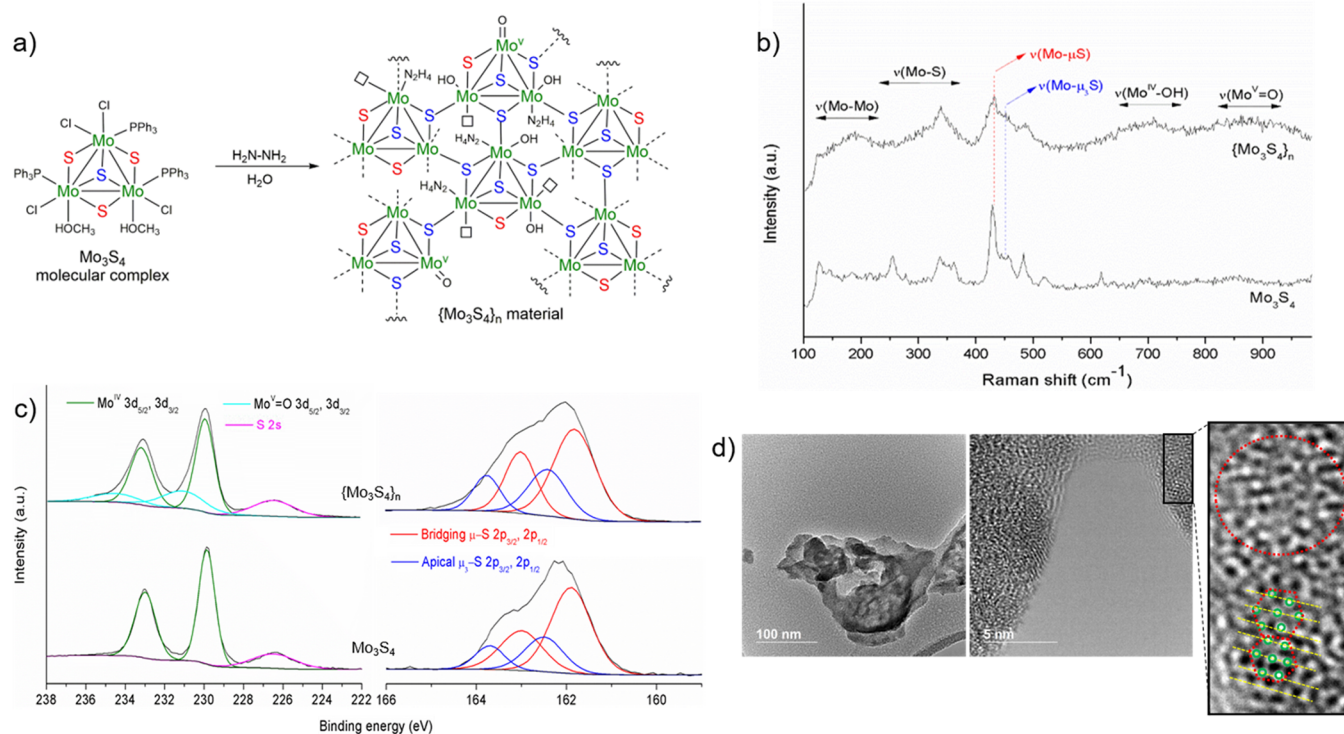


**Figure 1.** (a) Synthesis of  $\{\text{Mo}_3\text{S}_4\}_n$  from molecular complexes. Raman (b) and XPS (c) spectra of the  $\text{Mo}_3\text{S}_4$  molecular complex and  $\{\text{Mo}_3\text{S}_4\}_n$  material. (d) Low- and high-resolution TEM images of  $\{\text{Mo}_3\text{S}_4\}_n$ . The red dashed areas show lattice-distorted (circle) and ordered (hexagons) zones on the basal planes.

tion,<sup>106–113</sup> it also shares behavioral catalytic patterns. This approach allows engineering an efficient catalyst, containing a high degree of active sites on the basal planes, for the first straightforward synthesis of 2-substituted benzimidazoles from *o*-dinitroarenes and aldehydes in the presence of molecular hydrogen.

## RESULTS AND DISCUSSION

### Preparation and Structural Characterization of Catalyst $\{\text{Mo}_3\text{S}_4\}_n$

The starting  $\text{Mo}_3\text{S}_4$  molecular complex used to synthesize our novel sulfur deficient  $\text{MoS}_2$ -type material, namely  $\{\text{Mo}_3\text{S}_4\}_n$ , features an apical sulfur atom ( $\mu_3\text{-S}$ ), three bridging sulfur ligands ( $\mu\text{-S}$ ), and three molybdenum atoms, these latter in a triangular arrangement (Figure 1a). The outer positions around the Mo sites are occupied by chloride and triphenylphosphine ligands. In addition, although it was first proposed to be a coordinatively unsaturated compound,<sup>114</sup> it is generally accepted that solvent molecules from the preparation procedure (i.e., MeOH) fill the remaining vacant coordination sites.<sup>115,116</sup> The substitutional lability of these ligands and the robustness of the  $\text{Mo}_3\text{S}_4$  cluster core prompted us to imagine this precursor as a convenient building block for the construction of a higher nuclearity material, retaining, in principle, the  $\text{Mo}_3\text{S}_4$  motif. To this end, hydrazine hydrate was added at room temperature into a green-colored dispersion of the molecular complex in water, which turned black over the course of the reaction (see the Experimental Details for details on the preparation). This process implies the chemical reduction of the molecular complex by hydrazine, thereby enabling the intercluster assembly by nucleophilic attack from the bridging sulfur ligands to the outer coordination sites of Mo atoms, whereby the  $\{\text{Mo}_3\text{S}_4\}_n$  material

is formed. It should be noted that although coordination chemistry involving  $\text{Mo}_3\text{S}_4$  molecular complexes has extensively been investigated, such a type of reaction remains unknown.

The X-ray diffraction (XRD) pattern of  $\{\text{Mo}_3\text{S}_4\}_n$ , dominated by the presence of three broad diffraction peaks centered at  $2\theta$  values of 13.1, 37.1, and 50.3, resembles that of the poor crystalline hexagonal structure of previously reported  $\text{MoS}_2$  (Figure SII).<sup>93</sup> Inductively coupled plasma optical emission spectrometry (ICP-OES) measurements in combination with elemental analysis performed on  $\{\text{Mo}_3\text{S}_4\}_n$  revealed a S/Mo molar ratio of 1.25, similar than that of the theoretical one of 1.33 in the molecular complex precursor. This result confirms that a negligible sulfur loss occurred under hydrazine treatment during the material preparation.

The preservation of the  $\text{Mo}_3\text{S}_4$  structural motif in the synthesized  $\{\text{Mo}_3\text{S}_4\}_n$  material was investigated by Raman spectroscopy. Remarkably, the Raman spectrum of this material exhibits the same Raman signatures as those of the starting molecular complex (Figure 1b). Besides Raman bands, characteristic of metallic bonds ( $\nu(\text{Mo-Mo})$ ) at 125–230  $\text{cm}^{-1}$  and molybdenum sulfide bonds ( $\nu(\text{Mo-S})$ ) at 240–384  $\text{cm}^{-1}$ , vibration bands of bridging sulfur ligands ( $\nu(\mu\text{-S-Mo})$ ) and the apical sulfur atom ( $\nu(\mu_3\text{-S-Mo})$ ) appear at 430 and 448  $\text{cm}^{-1}$ , respectively.<sup>117,118</sup> Importantly, a decrease of the band intensity ratio of bridging to apical sulfides is observed in the spectrum of  $\{\text{Mo}_3\text{S}_4\}_n$  as result of the transformation from one to the other, whereby the intercluster assembly takes place. Additional broad bands centered at around 710 and 880  $\text{cm}^{-1}$  indicate the presence of  $\text{Mo}^{\text{IV}}\text{-OH}$  and  $\text{Mo}^{\text{V}}\text{=O}$  species, respectively.<sup>117,119,120</sup>

The chemical composition of  $\{\text{Mo}_3\text{S}_4\}_n$  was further verified by X-ray photoelectron spectroscopy (XPS; Figure 1c). The high-resolution S 2p core-level spectra of both the molecular complex



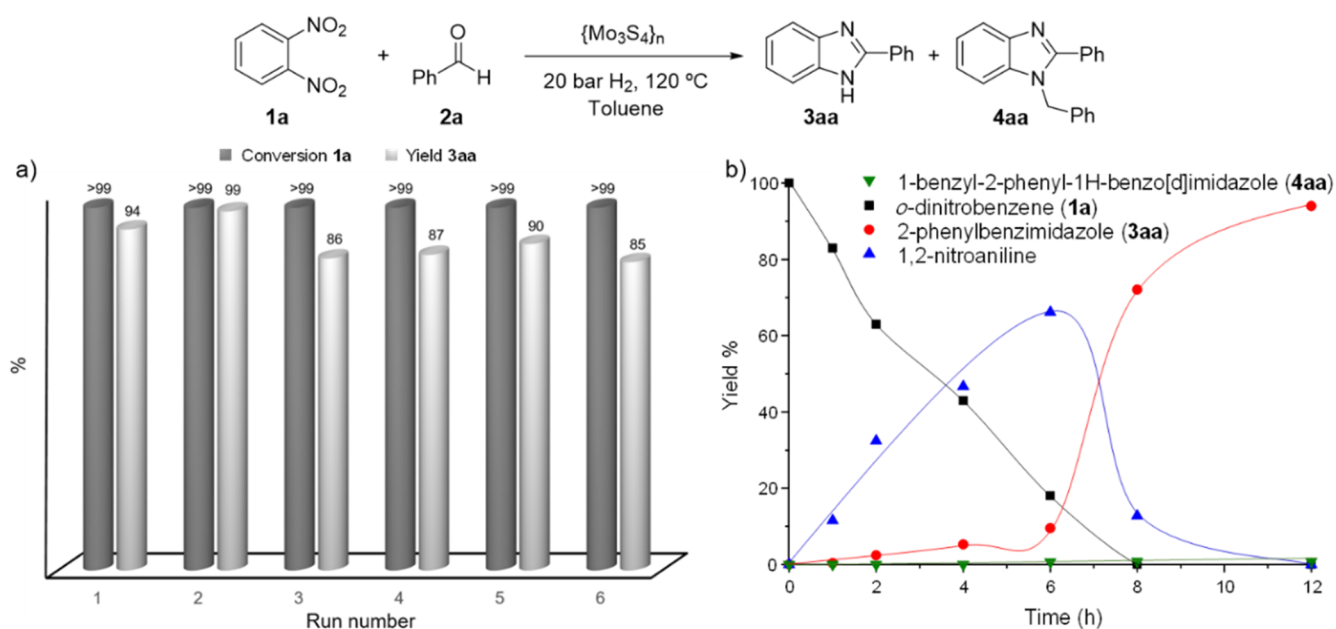


**Figure 2.** Catalyst recycling experiments (a) and reaction profile versus time (b) for the hydrogenative coupling of *o*-dinitrobenzene (**1a**) with benzaldehyde (**2a**) in the presence of catalyst  $\{\text{Mo}_3\text{S}_4\}_n$ . Reaction conditions: **1a** (0.25 mmol), **2a** (0.375 mmol),  $\{\text{Mo}_3\text{S}_4\}_n$  (10 mg), toluene (2 mL), 20 bar  $\text{H}_2$ , 120 °C, 16 h. Traces (<3%) of product **4aa** were detected in all reaction runs.

precursor and the  $\{\text{Mo}_3\text{S}_4\}_n$  material could be fitted into two sets of doublets, each of them characteristic of the spin–orbit splitting of S  $2p_{3/2}$  and S  $2p_{1/2}$  orbitals. The doublet at binding energies (BEs) of 161.9/163.0 eV is associated with the bridging sulfur ligands ( $\mu$ -S) and the other one at 162.5/163.7 eV with the apical sulfur atom ( $\mu_3$ -S).<sup>121</sup> Nevertheless, different percentages of each type of sulfur atoms were ascertained. Whereas the bridging and apical signals of the molecular complex precursor have a 77:23 area ratio, a higher contribution of the components associated with the apical sulfur atom (67:33) was found for  $\{\text{Mo}_3\text{S}_4\}_n$ .

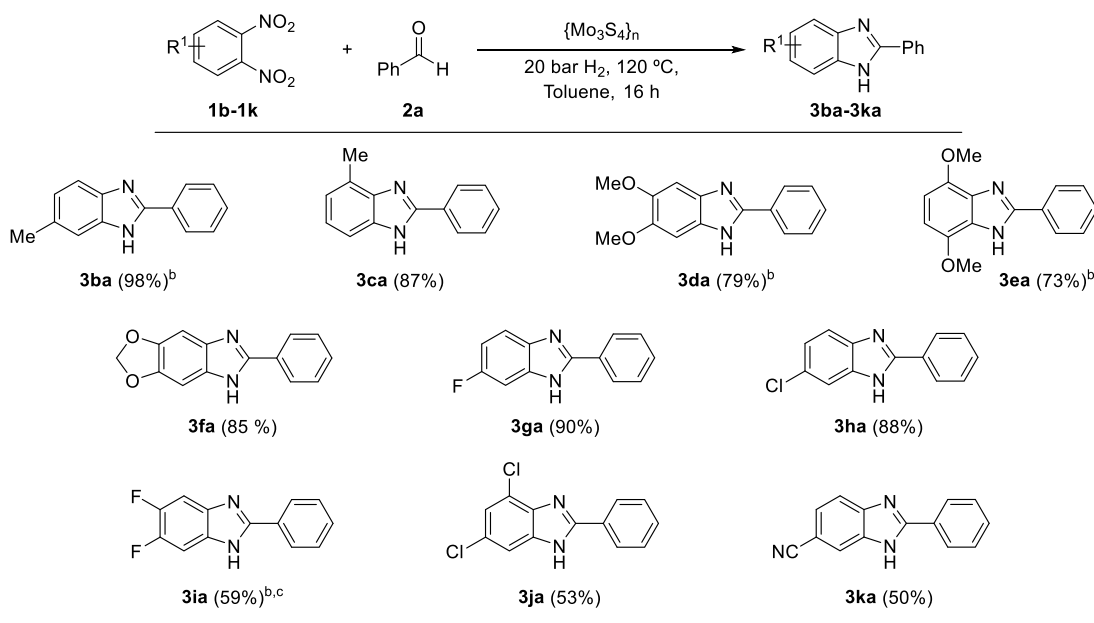
The high-resolution Mo 3d core-level spectra showed in both cases two peaks at 229.9 and 233.0 eV corresponding to the Mo  $3d_{5/2}$  and Mo  $3d_{3/2}$  orbitals, respectively, characteristic of Mo(IV) species. Moreover, for the  $\{\text{Mo}_3\text{S}_4\}_n$  material an additional doublet with a minor contribution at 230.9 and 234.4 eV was also detected after deconvolution and fitting, which could be ascribed to the presence of molybdenum oxysulfides ( $\text{Mo}^{\text{v}}\text{O}_x\text{S}_y$ ),<sup>117</sup> in good agreement with the Raman characterization results. Remarkably, the XPS survey spectrum of  $\{\text{Mo}_3\text{S}_4\}_n$  revealed the absence of Cl and P peaks but proved the presence of N (Figure S12). This observation suggests that chloride and triphenylphosphine ligands were fully removed during the intercluster assembly and that some hydrazine molecules lie in the structure, likely occupying remaining vacant coordination sites around Mo atoms.

The morphology and atomic structure of  $\{\text{Mo}_3\text{S}_4\}_n$  were investigated by transmission electron microscopy (TEM) at different magnifications (Figure 1d; see Figure S13 for HAADF-STEM and EDS elemental mapping characterization). The obtained images revealed that  $\{\text{Mo}_3\text{S}_4\}_n$  comprises randomly agglomerated nanosheets that preferentially expose their basal planes. The atomic structure of these basal planes is short-range ordered but long-range disordered with some regions displaying a hexagonal atomic arrangement of Mo atoms characteristic of a well-crystallized phase, but in general, they are mainly constituted by lattice-distorted zones. Consequently, such an

imperfect structure configuration implies the presence of active sites on the naturally occurring edge positions as well as along the typically inactive basal planes, thereby giving rise to a sulfur-deficient  $\text{MoS}_2$ -type catalyst that may display an excellent catalytic activity.

#### Catalytic Results for the Model Reaction

The hydrogenative reductive coupling of 1,2-dinitrobenzene (**1a**) with benzaldehyde (**2a**) for synthesizing 2-phenylbenzimidazole (**3aa**) was selected as a model reaction to demonstrate the performance of our  $\{\text{Mo}_3\text{S}_4\}_n$  material as a catalyst for this type of one-pot reaction sequence that involves the hydrogenation of nitro groups and the formation of C–N bonds, including a cyclization process. Initial experiments were performed in toluene at 100 °C and under 10 bar  $\text{H}_2$  pressure, conditions whereby **1a** was almost fully converted (in 94%) into 1,2-nitroaniline and **3aa** in 81 and 13% yield, respectively. Gratifyingly, pressure and temperature were shown to have a high impact on the efficiency of the reaction toward the formation of the desired benzimidazole product **3aa** (Table S11). In fact, by increasing the temperature up to 120 °C and/or the pressure up to 20 bar  $\text{H}_2$ , full conversion of **1a** was achieved affording **3aa** from 89 to 97% yield together with traces (<3%) of 1-benzyl-2-phenyl-1H-benzo[d]imidazole (**4aa**) as a byproduct. Surprisingly, besides traces of nonreacted benzaldehyde and its hydrogenated/oxidized derived compounds (i.e., benzyl alcohol and benzoic acid, respectively), small amounts of benzalazine, which is a byproduct that may be generated by dehydration reaction between benzaldehyde and hydrazine, were also detected (Scheme S11). This result supports the idea that some of the hydrazine used in the preparation of catalyst  $\{\text{Mo}_3\text{S}_4\}_n$  remains in its structure and justifies the observation of the N peak in the XPS survey spectrum (Figure S12). The use of other solvents was also investigated (Table S12). Whereas 1,4-dioxane led to lower reactivity, full conversion of **1a** and good to excellent yields of the desired benzimidazole **3aa**, but slightly lower than with toluene, were reached by using THF,  $\text{CH}_3\text{CN}$ , EtOH, and *i*PrOH. Further catalytic reactions were performed

**Scheme 2.  $\{\text{Mo}_3\text{S}_4\}_n$ -Catalyzed Synthesis of Benzimidazoles by Hydrogenative Coupling of Various *o*-Dinitroarene Derivatives with Benzaldehyde<sup>4a</sup>**


<sup>a</sup>Reaction conditions: 1b–1k (0.25 mmol), 2a (0.375 mmol),  $\{\text{Mo}_3\text{S}_4\}_n$  (10 mg), toluene (2 mL), 20 bar  $\text{H}_2$ , 120 °C, 16 h. <sup>b</sup> $\{\text{Mo}_3\text{S}_4\}_n$  (15 mg). <sup>c</sup>140 °C. Yields of isolated products are given.

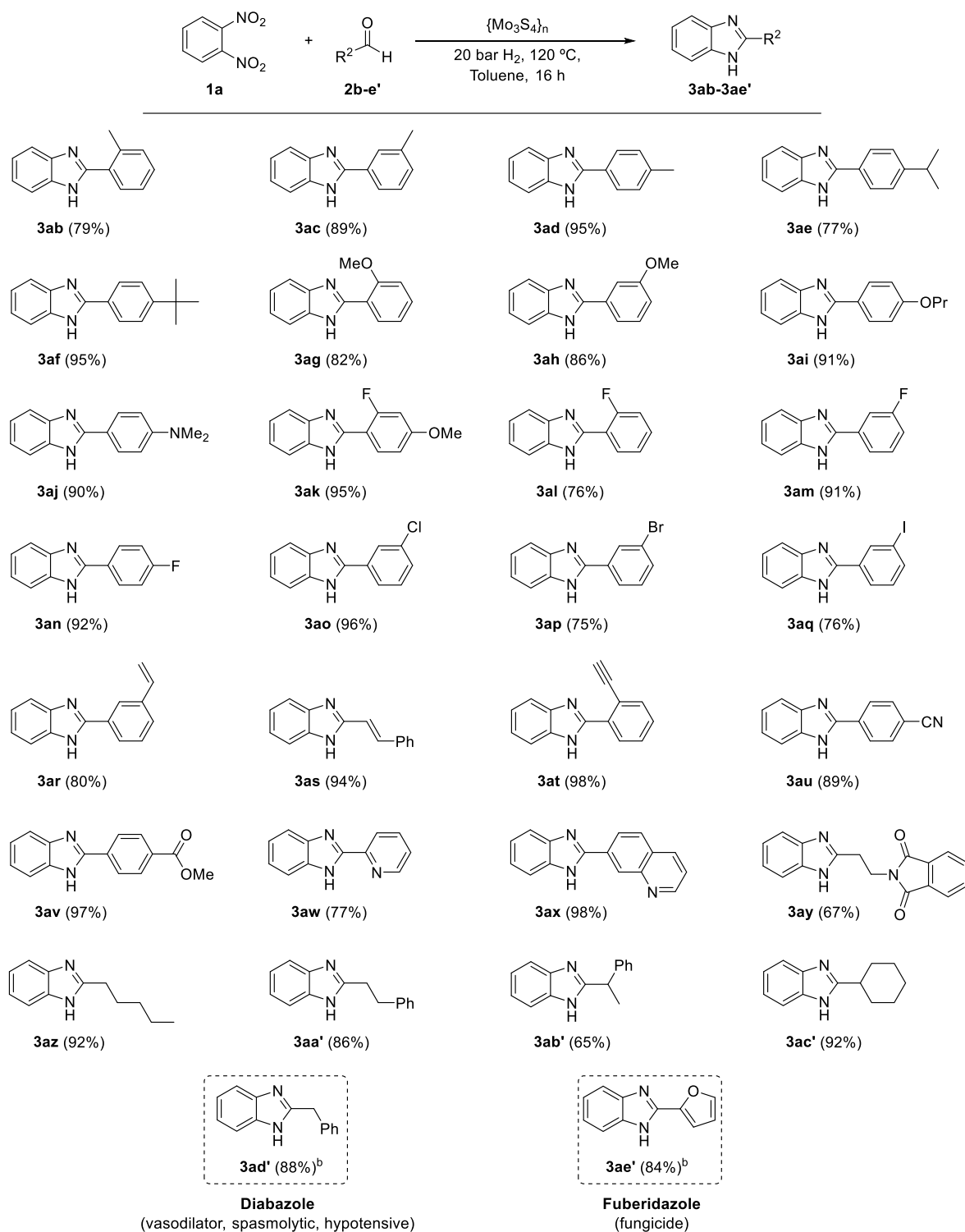
to optimize the catalyst loading, which could be halved with no significant influence on the yield of the desired benzimidazole product 3aa (Table S13).

To confirm the importance of presenting structural defects derived from the  $\text{Mo}_3\text{S}_4$ -type extended structure of  $\{\text{Mo}_3\text{S}_4\}_n$ , we prepared another material, namely, S- $\{\text{Mo}_3\text{S}_4\}_n$  from the same molecular complex precursor but under hydrothermal sulfurization conditions at 180 °C (see the Supporting Information for details on the preparation and characterization). The sulfurized material S- $\{\text{Mo}_3\text{S}_4\}_n$  with a S/Mo molar ratio of 1.74, comprises stacked nanosheets constituted by a hexagonal (2H)–trigonal (1T) mixed-phase of  $\text{MoS}_2$  and nonsulfurized  $\text{Mo}_3\text{S}_4$  domains to a lesser extent (Figures S14–S17). This structure configuration results in a catalyst that, compared with  $\{\text{Mo}_3\text{S}_4\}_n$ , displays a lesser defect-rich structure along basal planes, which, in addition, are less accessible to the reactants. In consequence, the sulfurized catalyst S- $\{\text{Mo}_3\text{S}_4\}_n$  exhibited a significant lower catalytic activity for the investigated tandem reaction (Figure S18). Likewise, when nondefective commercially available crystalline  $\text{MoS}_2$  was used as a catalyst, no reaction at all took place (Scheme S12).

The catalyst  $\{\text{Mo}_3\text{S}_4\}_n$  was proven to have good recyclability for the model reaction, achieving full conversion of 1a and excellent yield of 3aa for six consecutive runs (Figure 2a). Notably, no byproduct derived from hydrazine was detected in the second and subsequent runs, thus indicating that hydrazine was fully removed from the catalyst structure in the first reaction. Characterization of the six-times-recycled catalyst by XRD, HRTEM, and HAADF-STEM showed no obvious structure modifications (Figures S19–20), which could be discerned through an accurate XPS investigation (Figure S11). More specifically, the high-resolution S 2p XPS core-level spectrum revealed that the recycled catalyst displayed a lower percentage of sulfur bridging ligands (~20% less) and the presence of a new band at 170.0 eV that may be attributed to physically adsorbed sulfate species derived from the partial elimination of these

bridging sulfide moieties.<sup>122</sup> This finding is consistent with a previous study made on  $\text{Mo}_3\text{S}_4$  complexes that proposes the bridging sulfur ligands as the active sites where  $\text{H}_2$  undergoes dissociative adsorption,<sup>113</sup> which makes these moieties rather than apical sulfur atoms more prone to be removed. Incidentally, the presence of molybdenum oxysulfides ( $\text{Mo}^{\text{V}}\text{O}_x\text{S}_y$ ) was also detected to a slightly higher extent in the high-resolution Mo 3d XPS core-level spectrum. In good agreement with the XPS results, a weakening of the Raman vibration band associated with the bridging sulfur ligands ( $\nu(\mu\text{-S}-\text{Mo})$ ) was sensed in the Raman spectrum of the six-times-recycled catalyst (Figure S112). However, the main Raman signatures of the  $\text{Mo}_3\text{S}_4$  motif were preserved, thus indicating no significant loss of the cluster-like structure of catalyst  $\{\text{Mo}_3\text{S}_4\}_n$  along the reaction runs. It should be noted that only residual Mo traces (<0.15 wt %), which resulted to be catalytically inactive (Figure S113), were found by ICP analysis into the cumulative reaction mixtures obtained from six consecutive runs.

The reaction monitoring over time (Figure 2b) showed that, as the conversion of 1,2-dinitrobenzene (1a) increases, 1,2-nitroaniline is formed as a primary product. After reaching a maximum, the concentration of 1,2-nitroaniline dropped in concomitance with the formation of 2-phenylbenzimidazole (3aa) with no detection of other reaction intermediates, thus suggesting that the hydrogenation of 1,2-nitroaniline entails a kinetically less favored reaction step than the subsequent ones. Further analysis of this reaction profile reveals that the hydrogenation of 1,2-nitroaniline takes place at a higher reaction rate than that of the starting dinitroarene 1a, and therefore, its accumulation along the reaction likely arises from a preferential adsorption of 1a on the catalyst surface. This result is in line with our previous work on the hydrogenation of dinitroarenes in the presence of a cobalt-promoted  $\text{MoS}_2$ -based catalyst, in which good yields of the partially hydrogenated nitroanilines were reported.<sup>93</sup>

**Scheme 3.  $\{\text{Mo}_3\text{S}_4\}_n$ -Catalyzed Synthesis of Benzimidazoles by Hydrogenative Coupling of *o*-Dinitrobenzene with Different Aldehydes<sup>a</sup>**


<sup>a</sup>Reaction conditions: **1a** (0.25 mmol), **2b-e'** (0.375 mmol),  $\{\text{Mo}_3\text{S}_4\}_n$  (10 mg), toluene (2 mL), 20 bar  $\text{H}_2$ , 120 °C, 16 h. <sup>b</sup>**1a** (5 mmol), **2d'-e'** (7.5 mmol),  $\{\text{Mo}_3\text{S}_4\}_n$  (200 mg), toluene (30 mL), 20 bar  $\text{H}_2$ , 140 °C, 16 h. Yields of isolated products are given.

From a mechanistic point of view, once 1,2-nitroaniline is formed, in addition to a condensation step with benzaldehyde, the synthesis of **3aa** should involve either the intermediacy of a hydroxylamine derivative, followed by cyclization and dehydration, or alternatively, the complete hydrogenation of the nitro

group to the amine functionality, cyclization, and dehydrogenation (Scheme S13).<sup>62</sup> Since a dehydrogenative step under  $\text{H}_2$  pressure is rare, the feasibility of this route was investigated by using *o*-phenylenediamine as reactant (Scheme S14). This control experiment was performed under optimized reaction

conditions but using a 5-fold excess of catalyst loading to emulate the transient nature of this intermediate when it is formed in-route from the dinitroarene substrate. Surprisingly, the desired benzimidazole product **3aa** was afforded in 56% yield, thereby indicating that in the presence of catalyst  $\{\text{Mo}_3\text{S}_4\}_n$  the occurrence of the dehydrogenative pathway is highly likely.

### Substrate Scope

Having established the optimized conditions and investigated the catalytic performance of  $\{\text{Mo}_3\text{S}_4\}_n$  for the model reaction, we were curious to examine the use of various *o*-dinitroarenes as starting reagents (Scheme 2). When methyl-substituted dinitroarenes were coupled with benzaldehyde, the corresponding benzimidazole products **3ba** and **3ca** were obtained in 98 and 87% isolated yields, respectively. Likewise, electron-rich dinitroarenes containing methoxy groups or a cyclic acetal also underwent this reaction in high yields (**3da**–**3fa**). The use of electron-deficient dinitroarenes was also explored, and a significant electronic effect in the presence of such a type of functional groups was observed. Whereas 2-benzyl-6-fluoro-1*H*-benzo[*d*]imidazole (**3ga**) and 2-benzyl-6-chloro-1*H*-benzo[*d*]imidazole (**3ha**) were achieved in nearly 90% isolated yields, the introduction of a second halogen atom or the presence of a nitrile group resulted in a slightly lower reactivity toward the formation of the desired benzimidazoles **3ia**–**3ka**, which were isolated in moderate yields (50–59%). It should be noted that no dehalogenated products were detected.

Next, the general applicability of this hydrogenative reductive coupling methodology was further investigated by reaction of *o*-dinitrobenzene with a broad range of aldehydes (Scheme 3). To our delight, irrespective of the electro-withdrawing or -donating nature of the functional groups attached to the aromatic aldehydes, an outstanding reactivity to furnish the desired N-heterocyclic ring construction was achieved. *o*-Dinitrobenzene (**1a**) was reductively coupled with alkyl-, alkoxy-, and dimethylamine-substituted aldehydes resulting in good to excellent yields of the expected benzimidazole products (**3ab**–**3aj**). Halogenated aldehydes, even the bromide and iodide derivatives, also reacted efficiently, and again, the halide groups were well tolerated (**3ak**–**3aq**). Importantly, the  $\{\text{Mo}_3\text{S}_4\}_n$  catalyst was demonstrated to be compatible with the presence of potentially reducible double (**3ar**–**3as**) and triple (**3at**) carbon–carbon bonds, nitrile (**3au**), and ester (**3av**) groups. Heterocyclic aldehydes displaying a pyridine (**3aw**)-, quinoline (**3ax**)-, or phthalimide (**3ay**)-type structure were also suitable reactants to accomplish the reductive coupling reaction. Furthermore, 2-substituted benzimidazoles derived from the use of linear (**3az**–**3aa'**), branched (**3ab'**) and cyclic aliphatic (**3ac'**) aldehydes as coupling reagents were also accessible in up to 92% yield.

Finally, having knowledge of the catalytic behavior of catalyst  $\{\text{Mo}_3\text{S}_4\}_n$ , preparative-scale synthesis of pharmaceutical as well as agrochemical products was conducted as a proof-of-applicability (Scheme 3). Diabazole (**3ad'**), a spasmolytic, vasodilator, and hypotensive drug with cardiovascular applications,<sup>25</sup> was synthesized by hydrogenative coupling of *o*-dinitrobenzene with 2-phenylacetaldehyde and isolated in 88% yield. Furthermore, the same synthetic strategy was successfully applied for the preparation of the fungicide Fuberidazole (**3ae'**), which is widely used in the farm sector for pre- and postharvest treatment to avoid diverse types of fungal diseases on fruits and vegetables.<sup>6</sup> Gratifyingly, the reaction of *o*-dinitrobenzene with

biomass-derived furfuraldehyde resulted in 84% yield of **3ae'** after isolation.

### CONCLUSION

In conclusion, we have established a molecular cluster-based synthetic strategy to engineer a sulfur-deficient  $\text{MoS}_2$ -type material from  $\text{Mo}_3\text{S}_4$  complexes as precursors. The resulting material comprises randomly agglomerated nanosheets that preserve the specific atomic arrangement of the cluster motif within a  $\text{Mo}_3\text{S}_4$ -type extended structure, which entails the presence of structural defects on the naturally occurring edge positions as well as along the typically inactive basal planes. This peculiar structure configuration has enabled its application as an effective catalyst for the development of the first direct synthesis of benzimidazoles by reductive coupling of *o*-dinitroarenes with aldehydes using molecular hydrogen as a clean reducing agent. The catalyst displays good recyclability, affording the desired benzimidazole products in high yield even after six consecutive reaction runs. A wide variety of functionalized 2-substituted benzimidazoles have been accessed in good to excellent yields, even those containing potentially reducible and sensitive functional groups, such as double and triple carbon–carbon bonds, nitrile and ester groups, and halogens as well as diverse types of heteroarenes. The synthetic value of this methodology has been further demonstrated by synthesizing bioactive compounds with pharmaceutical and agrochemical applications. It is worth mentioning that the present catalytic methodology offers an attractive straightforward synthesis of benzimidazoles from cheap and readily available organic compounds using hydrogen as the reducing agent and a non-noble metal-based catalyst, thus constituting an environmentally benign way to access such a type of N-heterocyclic compounds in terms of compactness, cost, and atom efficiency. Moreover, the reported catalyst synthetic strategy could open a new avenue to engineer  $\text{MoS}_2$ -based materials with improved catalytic activity for organic chemistry, among others.

### EXPERIMENTAL DETAILS

#### Synthesis of $\text{Mo}_3\text{S}_4(\text{PPh}_3)_3\text{Cl}_4(\text{MeOH})_2$

The  $\text{Mo}_3\text{S}_4$  molecular complex was prepared following a slightly modified procedure with respect to the method reported in the literature.<sup>14</sup> Briefly, a 100 mL Schlenk flask containing a stirring bar was charged under nitrogen with  $(n\text{-Bu}_4\text{N})_2[\text{Mo}_3\text{S}_7\text{Cl}_6]$  (2 g) and methanol (50 mL) as a solvent. After stirring to dissolve the solid, triphenylphosphine (2.9 g) was added. A color change was observed from orange to green. The mixture was stirred for 20 min at room temperature. After this time, the mixture was filtered under vacuum, and the recovered solid was washed using a mixture of cold *n*-hexane:toluene (1:1) and then with hot *n*-hexane. Finally, the obtained green solid was allowed to dry under ambient conditions.

#### Preparation of Catalyst $\{\text{Mo}_3\text{S}_4\}_n$

$\text{Mo}_3\text{S}_4(\text{PPh}_3)_3\text{Cl}_4(\text{MeOH})_2$  (900 mg) was dispersed in distilled water (120 mL) into a beaker. Then, hydrazine monohydrate (64–65%, 6 mL) was slowly added under stirring conditions. A color change was observed from green to black. The mixture was stirred for 45 min at room temperature. After this time, the mixture was filtered under vacuum, and the recovered solid was washed using plenty of water, ethanol, and diethyl ether. Finally, the obtained black powder was allowed to dry under ambient conditions and stored under nitrogen atmosphere.

#### Preparation of Catalyst S- $\{\text{Mo}_3\text{S}_4\}_n$

S- $\{\text{Mo}_3\text{S}_4\}_n$  was prepared by a hydrothermal sulfurization process from the  $\text{Mo}_3\text{S}_4$  molecular complex in a 130 mL Parr stirred reactor.



$\text{Mo}_3\text{S}_4(\text{PPh}_3)_3\text{Cl}_4(\text{MeOH})_2$  (600 mg), sulfur (83.2 mg), distilled water (57 mL), and hydrazine monohydrated (64–65%, 5.5 mL) were introduced in a stainless steel autoclave vessel. Then, the autoclave was closed tightly and purged twice with nitrogen for leak testing. The mixture was heated and stirred until the desired internal temperature (180 °C) was reached and then maintained under static conditions at this temperature. After 22 h, the autoclave was cooled down to room temperature, and the generated gas was carefully released. The reaction mixture was filtered, and the recovered solid was washed with distilled water, ethanol, and diethyl ether. Finally, the obtained black solid was dried under ambient conditions and stored under a nitrogen atmosphere.

### General Procedure for the Synthesis of 2-Substituted Benzimidazoles by Hydrogenative Coupling of *o*-Dinitroarenes with Aldehydes

An 8 mL glass vial containing a stirring bar was charged with the corresponding *o*-dinitroarene (0.25 mmol), the aldehyde (1.5 equiv), the catalyst  $\{\text{Mo}_3\text{S}_4\}_n$  (10 mg), dodecane (50  $\mu\text{L}$ ) as internal standard, and toluene (2 mL) as a solvent. Then, the reaction vial was capped with a septum equipped with a syringe and placed in an alloy plate, which was then introduced into a 300 mL autoclave. Once sealed, the autoclave was purged with 30 bar  $\text{H}_2$  (3 times), then pressurized to 20 bar  $\text{H}_2$ , and placed into a preheated aluminum block located on a heating plate, which was previously set to 120 °C and 750 rpm of stirring speed. After 16 h, the autoclave was cooled down to room temperature and carefully depressurized. The reaction mixture was diluted with ethanol and an aliquot was taken for GC analysis. Finally, the product was purified by silica gel column chromatography (*n*-hexane/ethyl acetate mixtures) to give the desired product.

Instead of using an 8 mL glass vial, the preparative-scale syntheses of benzimidazoles were carried in a 50 mL round-bottom flask containing a stirring bar, which was charged with *o*-dinitrobenzene (5 mmol), the aldehyde (1.5 equiv), the catalyst  $\{\text{Mo}_3\text{S}_4\}_n$  (200 mg), and toluene (30 mL) as a solvent. The catalytic reaction was run at 140 °C, and the other experimental procedure was the same as described above.

## ■ ASSOCIATED CONTENT

### Supporting Information

The Supporting Information is available free of charge at <https://pubs.acs.org/doi/10.1021/jacsau.1c00477>.

General information on methods for characterization, additional characterization of the catalysts  $\{\text{Mo}_3\text{S}_4\}_n$  and S- $\{\text{Mo}_3\text{S}_4\}_n$ , extended data for catalytic experiments, characterization of the recycled catalyst, and leaching experiment, characterization data of isolated benzimidazoles (PDF)

## ■ AUTHOR INFORMATION

### Corresponding Authors

**Avelino Corma** – Instituto de Tecnología Química-Universitat Politècnica de València-Consejo Superior de Investigaciones Científicas (UPV-CSIC), 46022 Valencia, Spain;  
orcid.org/0000-0002-2232-3527; Email: [acorma@itq.upv.es](mailto:acorma@itq.upv.es)

**Iván Sorribes** – Instituto de Tecnología Química-Universitat Politècnica de València-Consejo Superior de Investigaciones Científicas (UPV-CSIC), 46022 Valencia, Spain;  
orcid.org/0000-0002-3721-9335; Email: [ivsorribes@itq.upv.es](mailto:ivsorribes@itq.upv.es)

### Authors

**Miriam Rodenes** – Instituto de Tecnología Química-Universitat Politècnica de València-Consejo Superior de Investigaciones Científicas (UPV-CSIC), 46022 Valencia, Spain

**Francisco Gonell** – Instituto de Tecnología Química-Universitat Politècnica de València-Consejo Superior de Investigaciones Científicas (UPV-CSIC), 46022 Valencia, Spain

**Santiago Martín** – Instituto de Nanociencia y Materiales de Aragón (INMA), CSIC, Universidad de Zaragoza, 50009 Zaragoza, Spain; Departamento de Química Física, Facultad de Ciencias, Universidad de Zaragoza, 50009 Zaragoza, Spain; orcid.org/0000-0001-9193-3874

Complete contact information is available at: <https://pubs.acs.org/doi/10.1021/jacsau.1c00477>

## Author Contributions

The manuscript was written through contributions of all authors. All authors have given approval to the final version of the manuscript.

## Notes

The authors declare no competing financial interest.

## ■ ACKNOWLEDGMENTS

This work has been supported by the Gen-T Plan of the Generalitat Valenciana through the “Subvencions a l’Excel·lència Científica de J únior s Investigadors” program (SEJI/2020/018). Financial support from the Spanish National Research Council (CSIC) is gratefully acknowledged (Project No. 201880E064). S.M. thanks for financial assistance from Ministerio de Ciencia e Innovación from Spain and fondos FEDER in the framework of the project PID2019-105881RB-I00 and DGA/fondos FEDER (construyendo Europa desde Aragón) for funding the research group Platón (E31\_17R). M.R. and F.G. acknowledge the Vice-Rectorate for Research, Innovation and Transfer of the Universitat Politècnica de València (UPV) for a pre- and postdoctoral (PAID-10-20) fellowship, respectively. The authors also thank the Electron Microscopy Service of the UPV for TEM and STEM facilities and Dr. G. Antorrena for technical support in XPS studies.

## ■ REFERENCES

- (1) Bhattacharya, S.; Chaudhuri, P. Medical Implications of Benzimidazole Derivatives as Drugs Designed for Targeting DNA and DNA Associated Processes. *Curr. Med. Chem.* **2008**, *15*, 1762–1777.
- (2) Preethi, P. J.; Karthikeyan, E.; Lohita, M.; Teja, P. G.; Subhash, M.; Shaheena, P.; Prashanth, Y.; Sai, N. K. Benzimidazole: An Important Scaffold in Drug Discovery. *Asian J. Pharm. Technol.* **2015**, *5*, 138–152.
- (3) Gaba, M.; Mohan, C. Development of Drugs Based on Imidazole and Benzimidazole Bioactive Heterocycles: Recent Advances and Future Directions. *Med. Chem. Res.* **2016**, *25*, 173–210.
- (4) Tahlan, S.; Kumar, S.; Narasimhan, B. Pharmacological Significance of Heterocyclic 1H-Benzimidazole Scaffolds: A Review. *BMC Chemistry* **2019**, *13*, 101.
- (5) Singh, N.; Pandurangan, A.; Rana, K.; Anand, P.; Ahamad, A.; Tiwari, A. K. Benzimidazole: A Short Review of Their Antimicrobial Activities. *Int. Curr. Pharm. J.* **2012**, *1*, 110–118.
- (6) Akhtar, W.; Khan, M. F.; Verma, G.; Shaquiquzzaman, M.; Rizvi, M. A.; Mehdi, S. H.; Akhter, M.; Alam, M. M. Therapeutic Evolution of Benzimidazole Derivatives in the Last Quinquennial Period. *Eur. J. Med. Chem.* **2017**, *126*, 705–753.
- (7) Akhtar, Md. J.; Yar, M. S.; Sharma, V. K.; Khan, A. A.; Ali, Z.; Haider, Md. R.; Pathak, A. Recent Progress of Benzimidazole Hybrids for Anticancer Potential. *Curr. Med. Chem.* **2020**, *27*, S970–6014.
- (8) Ermler, S.; Scholze, M.; Kortenkamp, A. Seven Benzimidazole Pesticides Combined at Sub-Threshold Levels Induce Micronuclei in Vitro. *Mutagenesis* **2013**, *28*, 417–426.



- (9) Weber, J. Nanostructured Poly(Benzimidazole): From Mesoporous Networks to Nanofibers. *ChemSusChem* **2010**, *3*, 181–187.
- (10) Jiang, J.-J.; Pan, M.; Liu, J.-M.; Wang, W.; Su, C.-Y. Assembly of Robust and Porous Hydrogen-Bonded Coordination Frameworks: Isomorphism, Polymorphism, and Selective Adsorption. *Inorg. Chem.* **2010**, *49*, 10166–10173.
- (11) Agarwal, R. A.; Aijaz, A.; Ahmad, M.; Sañudo, E. C.; Xu, Q.; Bharadwaj, P. K. Two New Coordination Polymers with Co(II) and Mn(II): Selective Gas Adsorption and Magnetic Studies. *Cryst. Growth Des.* **2012**, *12*, 2999–3005.
- (12) Tan, S.; Wei, B.; Liang, T.; Yang, X.; Wu, Y. Anhydrous Proton Conduction in Liquid Crystals Containing Benzimidazole Moieties. *RSC Adv.* **2016**, *6*, 34038–34042.
- (13) Saltan, G. M.; Dinçalp, H.; Kiran, M.; Zafer, C.; Erbaş, S. Ç. Novel Organic Dyes Based on Phenyl-Substituted Benzimidazole for Dye Sensitized Solar Cells. *Mater. Chem. Phys.* **2015**, *163*, 387–393.
- (14) Zhao, Y.; Wu, C.; Qiu, P.; Li, X.; Wang, Q.; Chen, J.; Ma, D. New Benzimidazole-Based Bipolar Hosts: Highly Efficient Phosphorescent and Thermally Activated Delayed Fluorescent Organic Light-Emitting Diodes Employing the Same Device Structure. *ACS Appl. Mater. Interfaces* **2016**, *8*, 2635–2643.
- (15) Wright, J. B. The Chemistry of the Benzimidazoles. *Chem. Rev.* **1951**, *48*, 397–541.
- (16) Preston, P. N. Synthesis, Reactions, and Spectroscopic Properties of Benzimidazoles. *Chem. Rev.* **1974**, *74*, 279–314.
- (17) Preston, P. N. In *Benzimidazoles and Congeneric Tricyclic Compounds, Part 2*; John Wiley & Sons: Chichester, 1980; pp 1–567.
- (18) Dudd, L. M.; Venardou, E.; Garcia-Verdugo, E.; Licence, P.; Blake, A. J.; Wilson, C.; Poliakoff, M. Synthesis of Benzimidazoles in High-Temperature Water. *Green Chem.* **2003**, *5*, 187–192.
- (19) Tandon, V. K.; Kumar, M. BF<sub>3</sub>·Et<sub>2</sub>O Promoted One-Pot Expeditious and Convenient Synthesis of 2-Substituted Benzimidazoles and 3,1,5-Benzoxadiazepines. *Tetrahedron Lett.* **2004**, *45*, 4185–4187.
- (20) Nadaf, R. N.; Siddiqui, S. A.; Daniel, T.; Lahoti, R. J.; Srinivasan, K. V. Room Temperature Ionic Liquid Promoted Regioselective Synthesis of 2-Aryl Benzimidazoles, Benzoxazoles and Benzthiazoles under Ambient Conditions. *J. Mol. Catal. A: Chem.* **2004**, *214*, 155–160.
- (21) Lin, S.-Y.; Isome, Y.; Stewart, E.; Liu, J.-F.; Yohannes, D.; Yu, L. Microwave-Assisted One Step High-Throughput Synthesis of Benzimidazoles. *Tetrahedron Lett.* **2006**, *47*, 2883–2886.
- (22) Wang, Y.; Sarris, K.; Sauer, D. R.; Djuric, S. W. A Simple and Efficient One Step Synthesis of Benzoxazoles and Benzimidazoles from Carboxylic Acids. *Tetrahedron Lett.* **2006**, *47*, 4823–4826.
- (23) Wang, R.; Lu, X.-x.; Yu, X.-q.; Shi, L.; Sun, Y. Acid-Catalyzed Solvent-Free Synthesis of 2-Arylbenzimidazoles under Microwave Irradiation. *J. Mol. Catal. A: Chem.* **2007**, *266*, 198–201.
- (24) Heravi, M. M.; Sadjadi, S.; Oskooie, H. A.; Shoar, R. H.; Bamoharram, F. F. Heteropolyacids as Heterogeneous and Recyclable Catalysts for the Synthesis of Benzimidazoles. *Catal. Commun.* **2008**, *9*, 504–507.
- (25) Alaqeel, S. I. Synthetic Approaches to Benzimidazoles from O-Phenylenediamine: A Literature Review. *J. Saudi Chem. Soc.* **2017**, *21*, 229–237.
- (26) Beaulieu, P. L.; Haché, B.; von Moos, E. A Practical Oxone®-Mediated, High-Throughput, Solution-Phase Synthesis of Benzimidazoles from 1,2-Phenylenediamines and Aldehydes and Its Application to Preparative Scale Synthesis. *Synthesis* **2003**, *2003*, 1683–1692.
- (27) Curini, M.; Epifano, F.; Montanari, F.; Rosati, O.; Taccone, S. Ytterbium Triflate Promoted Synthesis of Benzimidazole Derivatives. *Synlett* **2004**, *2004*, 1832–1834.
- (28) Gogoi, P.; Konwar, D. An Efficient and One-Pot Synthesis of Imidazolines and Benzimidazoles Via Anaerobic Oxidation of Carbon–Nitrogen Bonds in Water. *Tetrahedron Lett.* **2006**, *47*, 79–82.
- (29) Bahrami, K.; Khodaei, M. M.; Kavianinia, I. H<sub>2</sub>O<sub>2</sub>/HCl as a New and Efficient System for Synthesis of 2-Substituted Benzimidazoles. *J. Chem. Res.* **2006**, *2006*, 783–784.
- (30) Trivedi, R.; De, S. K.; Gibbs, R. A. A Convenient One-Pot Synthesis of 2-Substituted Benzimidazoles. *J. Mol. Catal. A: Chem.* **2006**, *245*, 8–11.
- (31) Bahrami, K.; Khodaei, M. M.; Kavianinia, I. A Simple and Efficient One-Pot Synthesis of 2-Substituted Benzimidazoles. *Synthesis* **2007**, *2007*, 547–550.
- (32) Chen, Y.-X.; Qian, L.-F.; Zhang, W.; Han, B. Efficient Aerobic Oxidative Synthesis of 2-Substituted Benzoxazoles, Benzothiazoles, and Benzimidazoles Catalyzed by 4-Methoxy-Tempo. *Angew. Chem., Int. Ed.* **2008**, *47*, 9330–9333.
- (33) Shingalapur, R. V.; Hosamani, K. M. An Efficient and Eco-Friendly Tungstate Promoted Zirconia (WO<sub>3</sub>/ZrO<sub>2</sub>) Solid Acid Catalyst for the Synthesis of 2-Aryl Benzimidazoles. *Catal. Lett.* **2010**, *137*, 63–68.
- (34) Narsaiah, A. V.; Reddy, A. R.; Yadav, J. S. Mild and Highly Efficient Protocol for the Synthesis of Benzimidazoles Using Samarium Triflate [Sm(OTf)<sub>3</sub>]. *Synth. Commun.* **2010**, *41*, 262–267.
- (35) Zhang, C.; Zhang, L.; Jiao, N. Catalyst Free Approach to Benzimidazoles Using Air as the Oxidant at Room Temperature. *Green Chem.* **2012**, *14*, 3273–3276.
- (36) Rojas-Buzo, S.; García-García, P.; Corma, A. Remarkable Acceleration of Benzimidazole Synthesis and Cyanosilylation Reactions in a Supramolecular Solid Catalyst. *ChemCatChem* **2017**, *9*, 997–1004.
- (37) Largeron, M.; Nguyen, K. M. H. Recent Advances in the Synthesis of Benzimidazole Derivatives from the Oxidative Coupling of Primary Amines. *Synthesis* **2018**, *50*, 241–253.
- (38) Sankar, V.; Karthik, P.; Neppolian, B.; Sivakumar, B. Metal–Organic Framework Mediated Expeditious Synthesis of Benzimidazole and Benzothiazole Derivatives through an Oxidative Cyclization Pathway. *New J. Chem.* **2020**, *44*, 1021–1027.
- (39) Kohli, S.; Rathee, G.; Hooda, S.; Chandra, R. Al<sub>2</sub>O<sub>3</sub>/Cui/Pani Nanocomposite Catalyzed Green Synthesis of Biologically Active 2-Substituted Benzimidazole Derivatives. *Dalton Trans.* **2021**, *50*, 7750–7758.
- (40) Climent, M. J.; Corma, A.; Iborra, S.; Martínez-Silvestre, S. Gold Catalysis Opens up a New Route for the Synthesis of Benzimidazolylquinoxaline Derivatives from Biomass-Derived Products (Glycerol). *ChemCatChem* **2013**, *5*, 3866–3874.
- (41) Daw, P.; Ben-David, Y.; Milstein, D. Direct Synthesis of Benzimidazoles by Dehydrogenative Coupling of Aromatic Diamines and Alcohols Catalyzed by Cobalt. *ACS Catal.* **2017**, *7*, 7456–7460.
- (42) Das, K.; Mondal, A.; Srimani, D. Selective Synthesis of 2-Substituted and 1,2-Disubstituted Benzimidazoles Directly from Aromatic Diamines and Alcohols Catalyzed by Molecularly Defined Nonphosphine Manganese(I) Complex. *J. Org. Chem.* **2018**, *83*, 9553–9560.
- (43) Li, L.; Luo, Q.; Cui, H.; Li, R.; Zhang, J.; Peng, T. Air-Stable Ruthenium(II)-NNN Pincer Complexes for the Efficient Coupling of Aromatic Diamines and Alcohols to 1H-Benzo[D]Imidazoles with the Liberation of H<sub>2</sub>. *ChemCatChem* **2018**, *10*, 1607–1613.
- (44) Chakrabarti, K.; Maji, M.; Kundu, S. Cooperative Iridium Complex-Catalyzed Synthesis of Quinoxalines, Benzimidazoles and Quinazolines in Water. *Green Chem.* **2019**, *21*, 1999–2004.
- (45) Tietze, L. F.; Beifuss, U. Sequential Transformations in Organic Chemistry: A Synthetic Strategy with a Future. *Angew. Chem., Int. Ed. Engl.* **1993**, *32*, 131–163.
- (46) Tietze, L. F.; Lieb, M. E. Domino Reactions for Library Synthesis of Small Molecules in Combinatorial Chemistry. *Curr. Opin. Chem. Biol.* **1998**, *2*, 363–371.
- (47) Tietze, L. F.; Modi, A. Multicomponent Domino Reactions for the Synthesis of Biologically Active Natural Products and Drugs. *Med. Res. Rev.* **2000**, *20*, 304–322.
- (48) Tietze, L. F.; Rackelmann, N. Domino Reactions in the Synthesis of Heterocyclic Natural Products and Analogs. *Pure Appl. Chem.* **2004**, *76*, 1967–1983.
- (49) Nicolaou, K. C.; Edmonds, D. J.; Bulger, P. G. Cascade Reactions in Total Synthesis. *Angew. Chem., Int. Ed.* **2006**, *45*, 7134–7186.
- (50) Tietze, L. F.; Brasche, G.; Gericke, K. In *Domino Reactions in Organic Synthesis*; Wiley-VCH: Weinheim, 2006; pp 1–10.

- (51) Climent, M. J.; Corma, A.; Iborra, S. Mono- and Multisite Solid Catalysts in Cascade Reactions for Chemical Process Intensification. *ChemSusChem* **2009**, *2*, 500–506.
- (52) Climent, M. J.; Corma, A.; Iborra, S. Heterogeneous Catalysts for the One-Pot Synthesis of Chemicals and Fine Chemicals. *Chem. Rev.* **2011**, *111*, 1072–1133.
- (53) Climent, M. J.; Corma, A.; Iborra, S.; Sabater, M. J. Heterogeneous Catalysis for Tandem Reactions. *ACS Catal.* **2014**, *4*, 870–891.
- (54) Feng, F.; Ye, J.; Cheng, Z.; Xu, X.; Zhang, Q.; Ma, L.; Lu, C.; Li, X. Cu–Pd/ $\gamma$ -Al<sub>2</sub>O<sub>3</sub> Catalyzed the Coupling of Multi-Step Reactions: Direct Synthesis of Benzimidazole Derivatives. *RSC Adv.* **2016**, *6*, 72750–72755.
- (55) Guan, Q.; Sun, Q.; Wen, L.; Zha, Z.; Yang, Y.; Wang, Z. The Synthesis of Benzimidazoles Via a Recycled Palladium Catalysed Hydrogen Transfer under Mild Conditions. *Org. Biomol. Chem.* **2018**, *16*, 2088–2096.
- (56) Feng, F.; Deng, Y.; Cheng, Z.; Xu, X.; Zhang, Q.; Lu, C.; Ma, L.; Li, X. Heterogeneous Catalytic Synthesis of 2-Methylbenzimidazole from 2-Nitroaniline and Ethanol over Mg Modified Cu–Pd/ $\gamma$ -Al<sub>2</sub>O<sub>3</sub>. *Catalysts* **2019**, *9*, 8.
- (57) Fukutake, T.; Wada, K.; Yu, H.; Hosokawa, S.; Feng, Q. Development of Titania-Supported Iridium Catalysts with Excellent Low-Temperature Activities for the Synthesis of Benzimidazoles Via Hydrogen Transfer. *Mol. Catal.* **2019**, *477*, 110550.
- (58) Das, S.; Mallick, S.; De Sarkar, S. Cobalt-Catalyzed Sustainable Synthesis of Benzimidazoles by Redox-Economical Coupling of O-Nitroanilines and Alcohols. *J. Org. Chem.* **2019**, *84*, 12111–12119.
- (59) Putta, R. R.; Chun, S.; Choi, S. H.; Lee, S. B.; Oh, D.-C.; Hong, S. Iron(0)-Catalyzed Transfer Hydrogenative Condensation of Nitroarenes with Alcohols: A Straightforward Approach to Benzoxazoles, Benzothiazoles, and Benzimidazoles. *J. Org. Chem.* **2020**, *85*, 15396–15405.
- (60) Yu, H.; Wada, K.; Fukutake, T.; Feng, Q.; Uemura, S.; Isoda, K.; Hirai, T.; Iwamoto, S. Effect of Phosphorus-Modification of Titania Supports on the Iridium-Catalyzed Synthesis of Benzimidazoles. *Catal. Today* **2021**, *375*, 410–417.
- (61) Wu, J.; Darcel, C. Iron-Catalyzed Hydrogen Transfer Reduction of Nitroarenes with Alcohols: Synthesis of Imines and Aza Heterocycles. *J. Org. Chem.* **2021**, *86*, 1023–1036.
- (62) Yang, D.; Fokas, D.; Li, J.; Yu, L.; Baldino, C. M. A Versatile Method for the Synthesis of Benzimidazoles from O-Nitroanilines and Aldehydes in One Step Via a Reductive Cyclization. *Synthesis* **2005**, *2005*, 47–56.
- (63) Schwob, T.; Kempe, R. A Reusable Co Catalyst for the Selective Hydrogenation of Functionalized Nitroarenes and the Direct Synthesis of Imines and Benzimidazoles from Nitroarenes and Aldehydes. *Angew. Chem., Int. Ed.* **2016**, *55*, 15175–15179.
- (64) Song, T.; Ren, P.; Duan, Y.; Wang, Z.; Chen, X.; Yang, Y. Cobalt Nanocomposites on N-Doped Hierarchical Porous Carbon for Highly Selective Formation of Anilines and Imines from Nitroarenes. *Green Chem.* **2018**, *20*, 4629–4637.
- (65) Bäumlner, C.; Kempe, R. The Direct Synthesis of Imines, Benzimidazoles and Quinoxalines from Nitroarenes and Carbonyl Compounds by Selective Nitroarene Hydrogenation Employing a Reusable Iron Catalyst. *Chem. - Eur. J.* **2018**, *24*, 8989–8993.
- (66) Ravi, K.; Advani, J. H.; Bankar, B. D.; Singh, A. S.; Biradar, A. V. Sustainable Route for the Synthesis of Flower-Like Ni@N-Doped Carbon Nanosheets from Bagasse and Its Catalytic Activity Towards Reductive Amination of Nitroarenes with Bio-Derived Aldehydes. *New J. Chem.* **2020**, *44*, 18714–18723.
- (67) Nguyen, T. B.; Ermolenko, L.; Al-Mourabit, A. Sodium Sulfide: A Sustainable Solution for Unbalanced Redox Condensation Reaction between O-Nitroanilines and Alcohols Catalyzed by an Iron–Sulfur System. *Synthesis* **2015**, *47*, 1741–1748.
- (68) Nguyen, T. B.; Le Bescont, J.; Ermolenko, L.; Al-Mourabit, A. Cobalt- and Iron-Catalyzed Redox Condensation of O-Substituted Nitrobenzenes with Alkylamines: A Step- and Redox-Economical Synthesis of Diazaheterocycles. *Org. Lett.* **2013**, *15*, 6218–6221.
- (69) Nguyen, T. B.; Ermolenko, L.; Corbin, M.; Al-Mourabit, A. Fe/S-Catalyzed Decarboxylative Redox Condensation of Arylacetic Acids with Nitroarenes. *Org. Chem. Front.* **2014**, *1*, 1157–1160.
- (70) Gan, H. Iron/S<sub>8</sub>-Catalyzed Redox Condensation of O-Nitroarenes with Arylmethyl Chloride: Synthesis of Benzimidazoles and Benzothiazoles. *Asian J. Org. Chem.* **2016**, *5*, 1111–1114.
- (71) Climent, M. J.; Corma, A.; Iborra, S.; Santos, L. L. Multisite Solid Catalyst for Cascade Reactions: The Direct Synthesis of Benzodiazepines from Nitro Compounds. *Chem. - Eur. J.* **2009**, *15*, 8834–8841.
- (72) Climent, M. J.; Corma, A.; Hernandez, J. C.; Hungria, A. B.; Iborra, S.; Martinez-Silvestre, S. Biomass into Chemicals: One-Pot Two- and Three-Step Synthesis of Quinoxalines from Biomass-Derived Glycols and 1,2-Dinitrobenzene Derivatives Using Supported Gold Nanoparticles as Catalysts. *J. Catal.* **2012**, *292*, 118–129.
- (73) Schwob, T.; Ade, M.; Kempe, R. A Cobalt Catalyst Permits the Direct Hydrogenative Synthesis of 1H-Perimidines from a Dinitroarene and an Aldehyde. *ChemSusChem* **2019**, *12*, 3013–3017.
- (74) Kim, J.; Kim, J.; Lee, H.; Lee, B. M.; Kim, B. H. Indium-Mediated One-Pot Benzimidazole Synthesis from 2-Nitroanilines or 1,2-Dinitroarenes with Orthoesters. *Tetrahedron* **2011**, *67*, 8027–8033.
- (75) Nagi Reddy, K. S.; Reddy, K. P.; Sabitha, G. Green Approach for the Domino Reduction/Reductive Amination of Nitroarenes and Chemoselective Reduction of Aldehydes Using Fe/Aq. Citric Acid/Montmorillonite K10. *ChemistrySelect* **2018**, *3*, 13670–13674.
- (76) Yu, L.; Zhang, Q.; Li, S.-S.; Huang, J.; Liu, Y.-M.; He, H.-Y.; Cao, Y. Gold-Catalyzed Reductive Transformation of Nitro Compounds Using Formic Acid: Mild, Efficient, and Versatile. *ChemSusChem* **2015**, *8*, 3029–3035.
- (77) Zhang, Q.; Li, S.-S.; Zhu, M.-M.; Liu, Y.-M.; He, H.-Y.; Cao, Y. Direct Reductive Amination of Aldehydes with Nitroarenes Using Bio-Renewable Formic Acid as a Hydrogen Source. *Green Chem.* **2016**, *18*, 2507–2513.
- (78) Topsøe, H.; Clausen, B. S.; Massoth, F. E. In *Hydrotreating Catalysis-Science and Technology* Anderson, J. R., Moudart, M., Eds.; Springer-Verlag: Berlin, 1996; Vol. 11; pp 1–269.
- (79) Toshiaki, K.; Atsushi, I.; Weihua, Q. In *Hydrodesulfurization and Hydrodenitrogenation: Chemistry and Engineering*; Wiley-VCH: Tokyo, 1999; pp 1–386.
- (80) Jaramillo, T. F.; Jorgensen, K. P.; Bonde, J.; Nielsen, J. H.; Horch, S.; Chorkendorff, I. Identification of Active Edge Sites for Electrochemical H<sub>2</sub> Evolution from MoS<sub>2</sub> Nanocatalysts. *Science* **2007**, *317*, 100–102.
- (81) Karunadasa, H. I.; Montalvo, E.; Sun, Y.; Majda, M.; Long, J. R.; Chang, C. J. A Molecular MoS<sub>2</sub> Edge Site Mimic for Catalytic Hydrogen Generation. *Science* **2012**, *335*, 698–702.
- (82) Kibsgaard, J.; Chen, Z.; Reinecke, B. N.; Jaramillo, T. F. Engineering the Surface Structure of MoS<sub>2</sub> To preferentially Expose Active Edge Sites For electrocatalysis. *Nat. Mater.* **2012**, *11*, 963.
- (83) Helveg, S.; Lauritsen, J. V.; Laegsgaard, E.; Stensgaard, I.; Nørskov, J. K.; Clausen, B. S.; Topsøe, H.; Besenbacher, F. Atomic-Scale Structure of Single-Layer MoS<sub>2</sub> Nanoclusters. *Phys. Rev. Lett.* **2000**, *84*, 951–954.
- (84) Lauritsen, J. V.; Bollinger, M. V.; Laegsgaard, E.; Jacobsen, K. W.; Nørskov, J. K.; Clausen, B. S.; Topsøe, H.; Besenbacher, F. Atomic-Scale Insight into Structure and Morphology Changes of MoS<sub>2</sub> Nanoclusters in Hydrotreating Catalysts. *J. Catal.* **2004**, *221*, 510–522.
- (85) Lauritsen, J. V.; Nyberg, M.; Nørskov, J. K.; Clausen, B. S.; Topsøe, H.; Laegsgaard, E.; Besenbacher, F. Hydrodesulfurization Reaction Pathways on MoS<sub>2</sub> Nanoclusters Revealed by Scanning Tunneling Microscopy. *J. Catal.* **2004**, *224*, 94–106.
- (86) Byskov, L. S.; Hammer, B.; Nørskov, J. K.; Clausen, B. S.; Topsøe, H. Sulfur Bonding in MoS<sub>2</sub> and Co-Mo-S Structures. *Catal. Lett.* **1997**, *47*, 177–182.
- (87) Lauritsen, J. V.; Kibsgaard, J.; Olesen, G. H.; Moses, P. G.; Hinnemann, B.; Helveg, S.; Nørskov, J. K.; Clausen, B. S.; Topsøe, H.; Laegsgaard, E.; Besenbacher, F. Location and Coordination of Promoter Atoms in Co- and Ni-Promoted MoS<sub>2</sub>-Based Hydrotreating Catalysts. *J. Catal.* **2007**, *249*, 220–233.



- (88) Topsøe, H. The Role of Co-Mo-S Type Structures in Hydrotreating Catalysts. *Appl. Catal., A* **2007**, *322*, 3–8.
- (89) Berhaut, G.; Perez De la Rosa, M.; Mehta, A.; Yácaman, M. J.; Chianelli, R. R. The Single-Layered Morphology of Supported MoS<sub>2</sub>-Based Catalysts—the Role of the Cobalt Promoter and Its Effects in the Hydrodesulfurization of Dibenzothiophene. *Appl. Catal., A* **2008**, *345*, 80–88.
- (90) Besenbacher, F.; Brorson, M.; Clausen, B. S.; Helveg, S.; Hinnemann, B.; Kibsgaard, J.; Lauritsen, J. V.; Moses, P. G.; Nørskov, J. K.; Topsøe, H. Recent STM, DFT and HAADF-STEM Studies of Sulfide-Based Hydrotreating Catalysts: Insight into Mechanistic, Structural and Particle Size Effects. *Catal. Today* **2008**, *130*, 86–96.
- (91) Kibsgaard, J.; Tuxen, A.; Knudsen, K. G.; Brorson, M.; Topsøe, H.; Lægsgaard, E.; Lauritsen, J. V.; Besenbacher, F. Comparative Atomic-Scale Analysis of Promotional Effects by Late 3d-Transition Metals in MoS<sub>2</sub> Hydrotreating Catalysts. *J. Catal.* **2010**, *272*, 195–203.
- (92) Zhu, Y.; Ramasse, Q. M.; Brorson, M.; Moses, P. G.; Hansen, L. P.; Kisielowski, C. F.; Helveg, S. Visualizing the Stoichiometry of Industrial-Style Co-Mo-S Catalysts with Single-Atom Sensitivity. *Angew. Chem., Int. Ed.* **2014**, *53*, 10723–10727.
- (93) Sorribes, I.; Liu, L.; Corma, A. Nanolayered Co-Mo-S Catalysts for the Chemoselective Hydrogenation of Nitroarenes. *ACS Catal.* **2017**, *7*, 2698–2708.
- (94) Sorribes, I.; Liu, L.; Doménech-Carbó, A.; Corma, A. Nanolayered Cobalt–Molybdenum Sulfides as Highly Chemo- and Regioselective Catalysts for the Hydrogenation of Quinoline Derivatives. *ACS Catal.* **2018**, *8*, 4545–4557.
- (95) Sorribes, I.; Corma, A. Nanolayered Cobalt–Molybdenum Sulphides (Co–Mo–S) Catalyze Borrowing Hydrogen C–S Bond Formation Reactions of Thiols or H<sub>2</sub>S with Alcohols. *Chem. Sci.* **2019**, *10*, 3130–3142.
- (96) To, T. A.; Nguyen, C. T.; Tran, M. H. P.; Huynh, T. Q.; Nguyen, T. T.; Le, N. T. H.; Nguyen, A. D.; Tran, P. D.; Phan, N. T. S. A New Pathway to Pyrrolo[1,2-a]Quinoxalines Via Solvent-Free One-Pot Strategy Utilizing Femose Nanosheets as Efficient Recyclable Synergistic Catalyst. *J. Catal.* **2019**, *377*, 163–173.
- (97) Zhang, C.; Zhang, Z.; Wang, X.; Li, M.; Lu, J.; Si, R.; Wang, F. Transfer Hydrogenation of Nitroarenes to Arylamines Catalysed by an Oxygen-Implanted MoS<sub>2</sub> Catalyst. *Appl. Catal., A* **2016**, *525*, 85–93.
- (98) Wang, J.; Zhang, Y.; Diao, J.; Zhang, J.; Liu, H.; Su, D. A MoS<sub>2</sub> Nanocatalyst with Surface-Enriched Active Sites for the Heterogeneous Transfer Hydrogenation of Nitroarenes. *Chin. J. Catal.* **2018**, *39*, 79–87.
- (99) Zhang, C.; Wang, X.; Li, M.; Zhang, Z.; Wang, Y.; Si, R.; Wang, F. Chemoselective Transfer Hydrogenation to Nitroarenes Mediated by Oxygen-Implanted MoS<sub>2</sub>. *Chin. J. Catal.* **2016**, *37*, 1569–1577.
- (100) Guardia, L.; Paredes, J. I.; Munuera, J. M.; Villar-Rodil, S.; Ayán-Varela, M.; Martínez-Alonso, A.; Tascón, J. M. D. Chemically Exfoliated MoS<sub>2</sub> Nanosheets as an Efficient Catalyst for Reduction Reactions in the Aqueous Phase. *ACS Appl. Mater. Interfaces* **2014**, *6*, 21702–21710.
- (101) García-Dalí, S.; Paredes, J. I.; Caridad, B.; Villar-Rodil, S.; Díaz-González, M.; Fernández-Sánchez, C.; Adawy, A.; Martínez-Alonso, A.; Tascón, J. M. D. Activation of Two-Dimensional MoS<sub>2</sub> Nanosheets by Wet-Chemical Sulfur Vacancy Engineering for the Catalytic Reduction of Nitroarenes and Organic Dyes. *Appl. Mater. Today* **2020**, *20*, 100678.
- (102) Srivastava, S. K.; Avasthi, B. N. Preparation and Characterization of Molybdenum-Disulfide Catalysts. *J. Mater. Sci.* **1993**, *28*, 5032–5035.
- (103) Sun, D.-Y.; Lin, B.-Z.; Xu, B.-H.; He, L.-W.; Ding, C.; Chen, Y.-L. Zr-Intercalated Molybdenum Disulfide: Preparation, Characterization and Catalytic Activity in Nitrobenzene Hydrogenation. *J. Porous Mater.* **2008**, *15*, 245–251.
- (104) Li, Z.; Zhang, D.; Ma, J.; Wang, D.; Xie, C. Fabrication of MoS<sub>2</sub> Microflowers for Hydrogenation of Nitrobenzene. *Mater. Lett.* **2018**, *213*, 350–353.
- (105) Zhang, Y.; Gao, Y.; Yao, S.; Li, S.; Asakura, H.; Teramura, K.; Wang, H.; Ma, D. Sublimation-Induced Sulfur Vacancies in MoS<sub>2</sub> Catalyst for One-Pot Synthesis of Secondary Amines. *ACS Catal.* **2019**, *9*, 7967–7975.
- (106) Sorribes, I.; Wienhoefer, G.; Vicent, C.; Junge, K.; Llusar, R.; Beller, M. Chemoselective Transfer Hydrogenation to Nitroarenes Mediated by Cubane-Type Mo<sub>3</sub>S<sub>4</sub> Cluster Catalysts. *Angew. Chem., Int. Ed.* **2012**, *51*, 7794–7798.
- (107) Pedrajas, E.; Sorribes, I.; Junge, K.; Beller, M.; Llusar, R. A Mild and Chemoselective Reduction of Nitro and Azo Compounds Catalyzed by a Well-Defined Mo<sub>3</sub>S<sub>4</sub> Cluster Bearing Diamine Ligands. *ChemCatChem* **2015**, *7*, 2675–2681.
- (108) Pedrajas, E.; Sorribes, I.; Gushchin, A. L.; Laricheva, Y. A.; Junge, K.; Beller, M.; Llusar, R. Chemoselective Hydrogenation of Nitroarenes Catalyzed by Molybdenum Sulphide Clusters. *ChemCatChem* **2017**, *9*, 1128–1134.
- (109) Pedrajas, E.; Sorribes, I.; Junge, K.; Beller, M.; Llusar, R. Selective Reductive Amination of Aldehydes from Nitro Compounds Catalyzed by Molybdenum Sulfide Clusters. *Green Chem.* **2017**, *19*, 3764–3768.
- (110) Pedrajas, E.; Sorribes, I.; Guillamón, E.; Junge, K.; Beller, M.; Llusar, R. Efficient and Selective N-Methylation of Nitroarenes under Mild Reaction Conditions. *Chem. - Eur. J.* **2017**, *23*, 13205–13212.
- (111) Algarra, A. G.; Guillamón, E.; Andrés, J.; Fernández-Trujillo, M. J.; Pedrajas, E.; Pino-Chamorro, J. Á.; Llusar, R.; Basallote, M. G. Cuboidal Mo<sub>3</sub>S<sub>4</sub> Clusters as a Platform for Exploring Catalysis: A Three-Center Sulfur Mechanism for Alkyne Semihydrogenation. *ACS Catal.* **2018**, *8*, 7346–7350.
- (112) Safont, V. S.; Sorribes, I.; Andrés, J.; Llusar, R.; Oliva, M.; Ryzhikov, M. R. On the Catalytic Transfer Hydrogenation of Nitroarenes by a Cubane-Type Mo<sub>3</sub>S<sub>4</sub> Cluster Hydride: Disentangling the Nature of the Reaction Mechanism. *Phys. Chem. Chem. Phys.* **2019**, *21*, 17221–17231.
- (113) Guillamón, E.; Oliva, M.; Andrés, J.; Llusar, R.; Pedrajas, E.; Safont, V. S.; Algarra, A. G.; Basallote, M. G. Catalytic Hydrogenation of Azobenzene in the Presence of a Cuboidal Mo<sub>3</sub>S<sub>4</sub> Cluster Via an Uncommon Sulfur-Based H<sub>2</sub> Activation Mechanism. *ACS Catal.* **2021**, *11*, 608–614.
- (114) Fedin, V. P.; Sokolov, M. N.; Mironov, Y. V.; Kolesov, B. A.; Tkachev, S. V.; Fedorov, V. Y. Triangular Thiocomplexes of Molybdenum - Reactions with Halogens, Hydrohalogen Acids and Phosphines. *Inorg. Chim. Acta* **1990**, *167*, 39–45.
- (115) Avarvari, N.; Kiracki, K.; Llusar, R.; Polo, V.; Sorribes, I.; Vicent, C. Hybrid Organic/Inorganic Complexes Based on Electroactive Tetrathiafulvalene-Functionalized Diphosphanes Tethered to C<sub>3</sub>-Symmetrized Mo<sub>3</sub>Q<sub>4</sub> (Q = S, Se) Clusters. *Inorg. Chem.* **2010**, *49*, 1894–1904.
- (116) Beltran, T. F.; Llusar, R.; Sokolov, M.; Basallote, M. G.; Fernandez-Trujillo, M. J.; Pino-Chamorro, J. A. Influence of the Ligand Alkyl Chain Length on the Solubility, Aqueous Speciation, and Kinetics of Substitution Reactions of Water-Soluble M<sub>3</sub>S<sub>4</sub> (M = Mo, W) Clusters Bearing Hydroxyalkyl Diphosphines. *Inorg. Chem.* **2013**, *52*, 8713–8722.
- (117) Tran, P. D.; Tran, T. V.; Orio, M.; Torelli, S.; Truong, Q. D.; Nayuki, K.; Sasaki, Y.; Chiam, S. Y.; Yi, R.; Honma, I.; Barber, J.; Artero, V. Coordination Polymer Structure and Revisited Hydrogen Evolution Catalytic Mechanism for Amorphous Molybdenum sulfide. *Nat. Mater.* **2016**, *15*, 640.
- (118) Deng, Y.; Ting, L. R. L.; Neo, P. H. L.; Zhang, Y.-J.; Peterson, A. A.; Yeo, B. S. Operando Raman Spectroscopy of Amorphous Molybdenum Sulfide (MoS<sub>x</sub>) During the Electrochemical Hydrogen Evolution Reaction: Identification of Sulfur Atoms as Catalytically Active Sites for H<sup>+</sup> Reduction. *ACS Catal.* **2016**, *6*, 7790–7798.
- (119) Hardcastle, F. D.; Wachs, I. E. Determination of Molybdenum–Oxygen Bond Distances and Bond Orders by Raman Spectroscopy. *J. Raman Spectrosc.* **1990**, *21*, 683–691.
- (120) Escalera-López, D.; Lou, Z.; Rees, N. V. Benchmarking the Activity, Stability, and Inherent Electrochemistry of Amorphous Molybdenum Sulfide for Hydrogen Production. *Adv. Energy Mater.* **2019**, *9*, 1802614.



(121) Ting, L. R. L.; Deng, Y.; Ma, L.; Zhang, Y.-J.; Peterson, A. A.; Yeo, B. S. Catalytic Activities of Sulfur Atoms in Amorphous Molybdenum Sulfide for the Electrochemical Hydrogen Evolution Reaction. *ACS Catal.* **2016**, *6*, 861–867.

(122) Huang, Y.; Sun, Y.; Zheng, X.; Aoki, T.; Pattengale, B.; Huang, J.; He, X.; Bian, W.; Younan, S.; Williams, N.; Hu, J.; Ge, J.; Pu, N.; Yan, X.; Pan, X.; Zhang, L.; Wei, Y.; Gu, J. Atomically Engineering Activation Sites onto Metallic 1T-MoS<sub>2</sub> Catalysts for Enhanced Electrochemical Hydrogen Evolution. *Nat. Commun.* **2019**, *10*, 982.